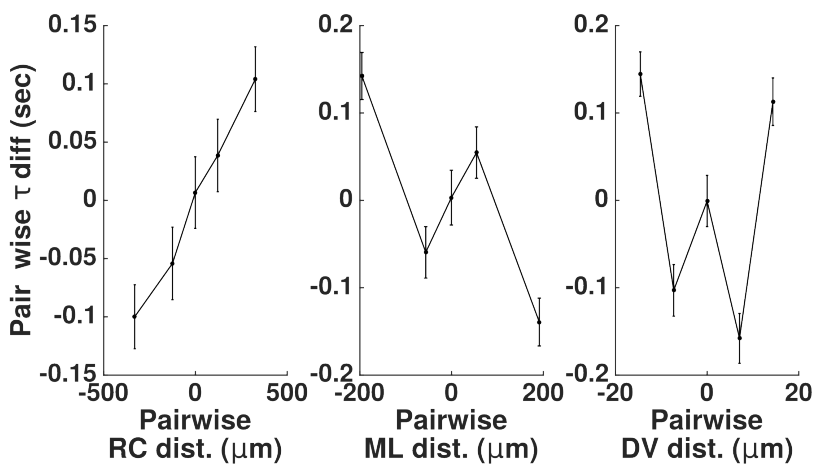


Supplementary information for Vishwanathan et al.

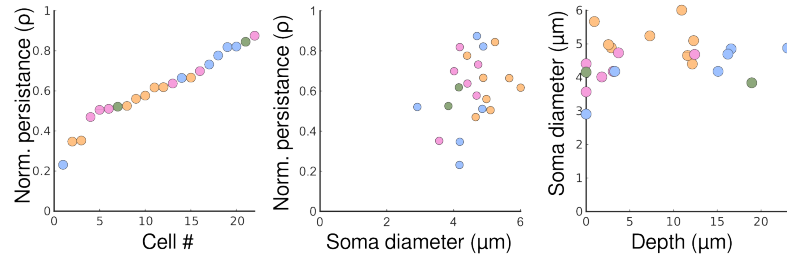
July 11, 2016

1 Supplementary figures

A



B



C

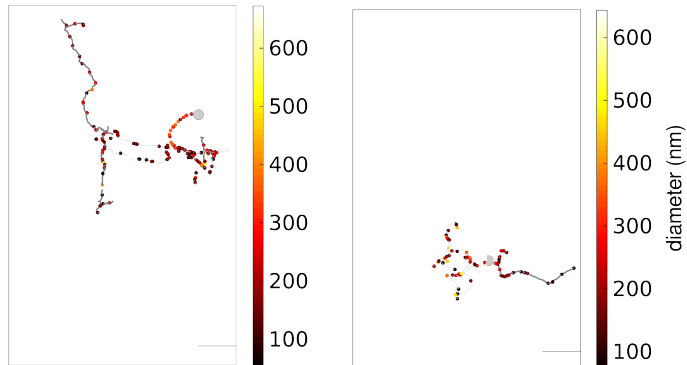


Figure 1: Supplementary figure 1

(A) Pairwise difference in time constants for all integrator neurons. Left, Pairwise difference of time constants of integrator neurons along the rostro-caudal axis. Rostral to the left and dorsal to the right. Middle, Pairwise difference of time constants along the medio-lateral axis. Right, pairwise difference of time constants along the dorso-ventral axis. All values reported as mean \pm SEM

(B) (left) Normalized persistence time measure for all cells in the study. Colors represent the group that the cell belong to. (Pink - ipsi only, Green - Ipsi-contra, Orange - contra only and Blue - unknown).

(middle) Normalized persistence time versus diameter of integrator cells somata.

(right) Integrator neuron soma diameter versus the depth along the dorso-ventral axis

(C) Diameter profiles along ipsi only (left) and contra only (right) integrator cells.

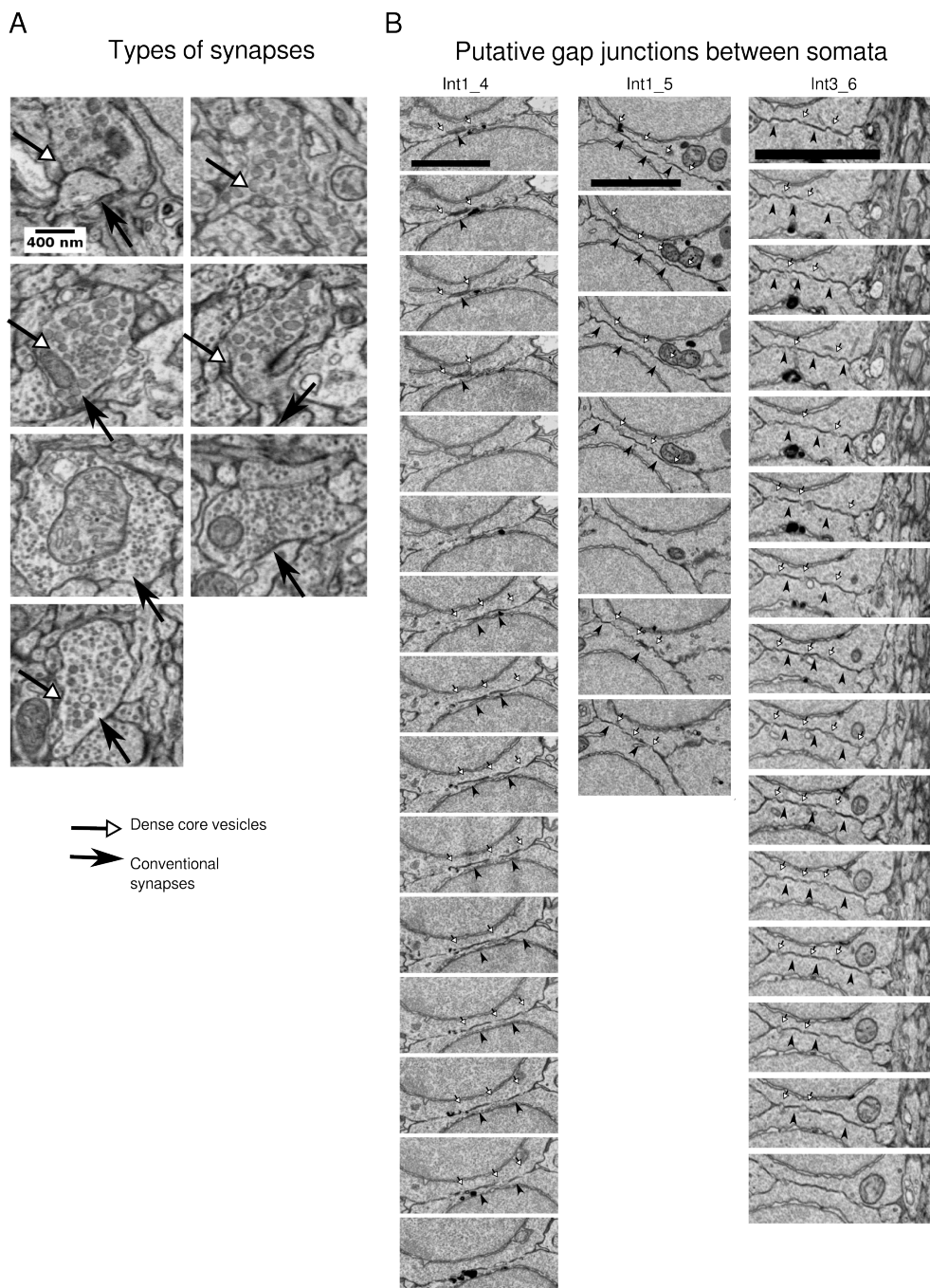


Figure 2: Supplementary figure 2

(A) Examples of types of synapses in the imaged volume. Closed arrows show conventional synapses and open arrows shows dense core vesicles within the same bouton.

(B) Successive images from putative tight junctions between cells somata. Closed arrow head shows tight juction indicated by darkening of the membrane in the same location in multiple sections. Open arrows show the separation of the membrane by the lack of darkening. Scale bar 500nm

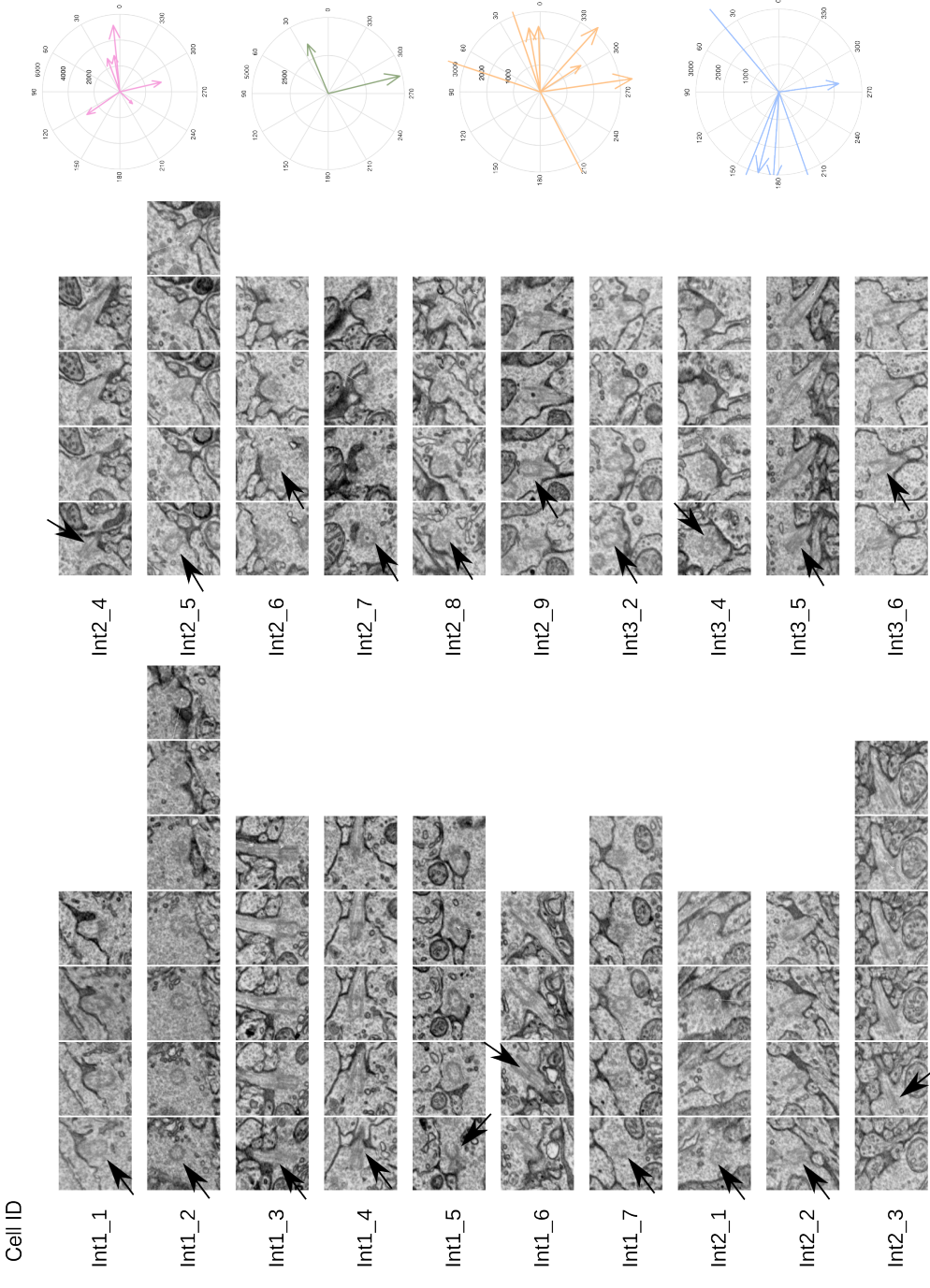


Figure 3: Supplementary figure 3
 (A) Primary cilium of every integrator cell identified in the volume. The primary cilium is visible in multiple sections by the presence of a microtubule rich neurite (arrow) that emerges very close to the Golgi complex of the cells.
 (B) Orientation of the primary cilium for the four cell groups.

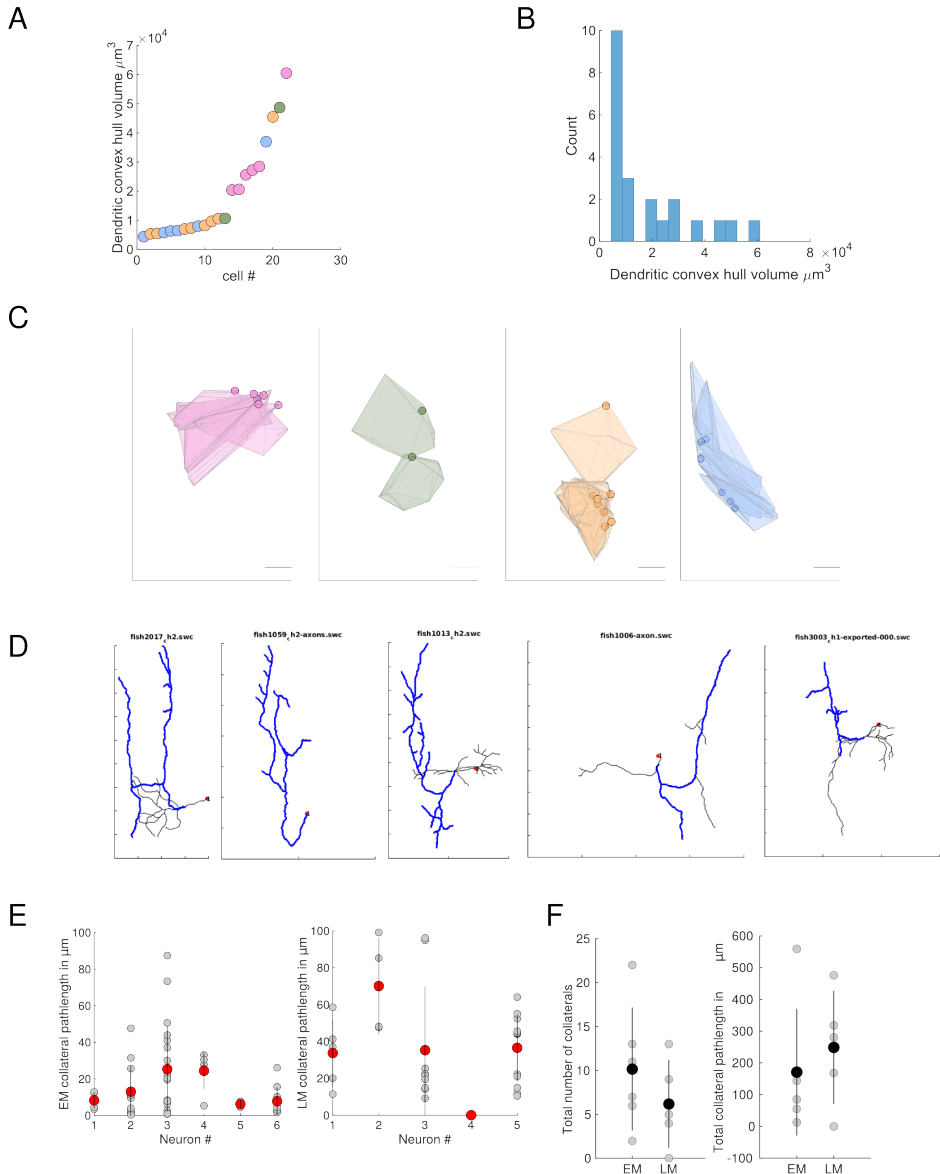


Figure 4: Supplementary figure 4

(A) Convex hull volume of dendrites of all integrator cells, color coded by the cell group that they belong to.

(B) Distribution of the convex hull volume of the integrator cells.

(C) Convex hulls of all cells color coded by the group that they belong to.

(D) Traces of integrator cells from light microscopic dye fills, with ipsilateral projecting axons that were used for comparison with EM cells.

(E) Collateral path length of all EM , LM cells respectively. Grey circles are for individual collaterals for each cells, and red circle is the mean \pm standard deviation.

(F) Number of Collaterals and pathlength of collaterals for EM and LM traces.

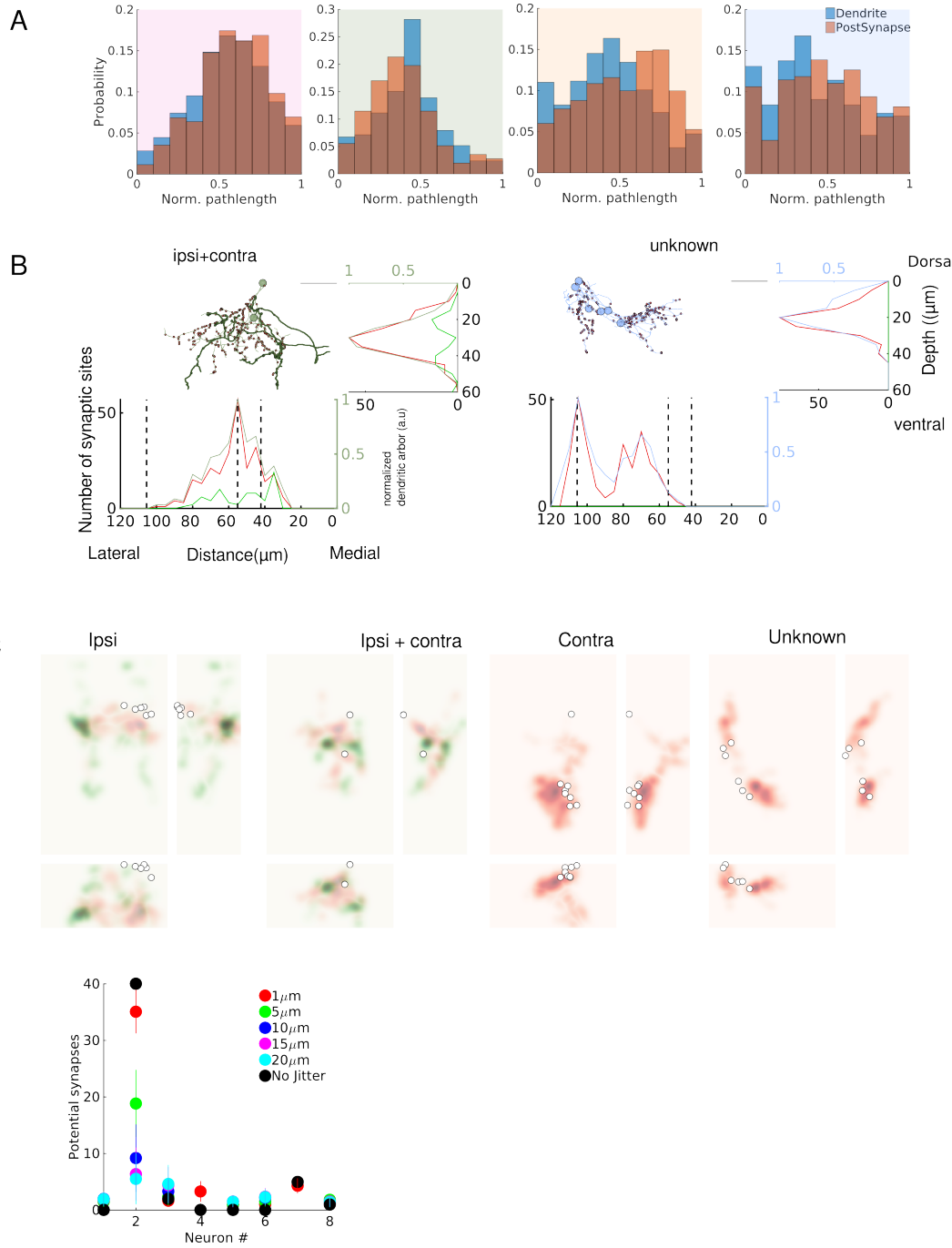


Figure 5: Supplementary figure 5

(A) Distribution of the normalized postsynaptic pathlength and the distribution of the normalized dendritic pathlength for all four groups.
 (B) Depth stratification of all cells in each group. For each panel, below the trace of all cells is the stratification of the dendrites (red) and axons (green) along the mediolateral axis. To the right is the stratification along the dorso-ventral axis. Black dotted line are the locations of the stripes from figure 4.
 (C) Normalized density plot of the pre and postsynaptic sites with somata of the cells indicated by white circles.
 (D) Jittering of the potential synapses for all integrator cells with axons.

Cell group	# Cells	Total length (μm)	Axonal length (μm)	Dendritic length (μm)	Convex hull volume (μm^3)	Axon diameters (μm)	Dendrite diameter (μm)
Ipsi. only	6	661.89 ± 253.57	269.74 ± 244.41	392.14 ± 66.31	3.04×10^4	0.21 ± 0.15	0.25 ± 0.15
Ipsi-contra.	2	696.59 ± 200.92	277.28 ± 22.08	419.30 ± 178.84	2.96×10^4	0.2 ± 0.11	0.21 ± 0.12
Contra. only	8	358.13 ± 62.76	65.72 ± 15.24	292.41 ± 69.75	1.23×10^4	0.16 ± 0.08	0.22 ± 0.12
unknown	6	221.47 ± 48.7	NA	221.47 ± 48.70	1.13×10^4	NA	0.22 ± 0.12

Table 1: Anatomical details

2 Supplementary table

3 Supplementary experimental procedure

Two-photon calcium imaging.

Nacre mutant zebrafish larvae, X days of age, was anesthetized in 100 or 200 mg/L tricaine-methanesulfonate (MS222, VWR TCT0941-025G) for about 1 minute and then quickly mounted dorsal side up with droplets of 1.7% low temperature agarose (Sigma A0701-100G) in the lid of a 35mm petri dish containing a bed of hardened 1% agarose (Invitrogen 15510-027). The larva was then covered in 50 mg/L MS222. The larva was bulk-loaded (**author?**) [1, 6] with calcium sensitive dye Oregon Green 488 BAPTA-1 AM (5 mM, in DMSO with 5% pluronic, Invitrogen, O-6807) by inserting a capillary through the dorsal skin surface over the lateral edge of the right side of the hindbrain just caudal to the cerebellum, at ~30° decline relative to the dorsal surface.

Briefly, a stack was acquired over the same imaging window, with optical sections every 1.3 μ m, and with a lateral resolution of 0.5 μ m. Once this was performed, the animal was anesthetized and the skin over the hindbrain was removed, to facilitate penetration of the fixative, and the animal was immersed in fixative to preserve the ultrastructure. We found that the removal of the skin was important for good quality fixation.

Serial section electron microscopy.

The animal was immersed in a fixative of 1% paraformaldehyde and 1% glutaraldehyde buffered in 0.1M cacodylate buffer for 24 hrs. Then it was thoroughly washed in 0.1M cacodylate buffer before staining. The tissue was stained using a conventional ROTO procedure ((**author?**) [7]). the tissue was infiltrated with an LX-112 based EPON resin for 24 hrs and baked for 48 hrs at 60 C. The EPON based resin was tailored to have low viscosity, to help with better infiltration for this tissue. Following hardening, the tissue block face was coarsely trimmed and a rectangular mesa was defined for serial sectioning. Care was taken to orient the specimen to permit sectioning along the horizontal axis. Serial sections from the above animal were collected approximately from the level of the Mauthner cell at a thickness of 45 nm. . The serial sections were then adhered to a silicon wafer, using double sided carbon tape (TEDpella), the wafers were coated with a thin film of carbon to make them conductive. Images were imported into the TrakEM2 framework and montaged, first, using affine transforms, followed by elastic transforms. The images were then registered using a similar approach, where the first pass was performed using affine transforms, followed by elastic transforms. All the alignment was performed on a machine with 32 cores and 120GB RAM.

3.1 Registration of light microscope and electron microscope volumes

We first performed functional imaging in an awake, immobilized larval zebrafish using the calcium sensitive dye OGB, by introducing the dye in the hindbrain via iontophoresis, similar to methods used previously [3, 5] . Once this was done, the animal was placed in an imaging setup that allowed for imaging the activity in the hindbrain, while simultaneously imaging the eye movement behavior. . This paradigm allows for the correlation of eye movement behavior to the firing of cells in the hindbrain. We performed the functional light microscopy at pre-defined planes close to and below the Mauthner cell unilaterally.

Once functional imaging of the larva was performed, it was immediately prepared for electron microscopy by immersing in fixative. The larva was processed for electron microscopy using conventional reduced osmium staining techniques and embedded in an epoxy based resin [7]. The tissue block was then coarsely trimmed until the appearance of the Mauthner cell plane. Following the observation of this landmark , ultra-thin sections (Fig. 1B, 1st panel) were collected in an automated manner using an automated tape collecting ultramicrotome (ATUM) as described previously [4]. The sections were then made conductive, by evaporating a thin layer of carbon and imaged in a field emitting scanning electron microscope (FE-SEM) to obtain an electron microscopy (EM) volume. Each section was imaged at a resolution of 5nm/pixel in a region of interest that roughly corresponded with area imaged on the light microscopic. The EM volume we imaged contained 15791 image tiles (8K x 8K pixels each) or $\sim 10^{11}$ pixels. These images were registered using the trakEM2 plugin in Fiji [2]. Briefly, individual images were first montaged using affine transforms followed by elastic transforms. Following this they were aligned in the z dimension, using first, affine and followed by elastic transforms.

To locate the cells that were involved in the integrator circuit, we first extracted the location of cells in the light microscopic volume that were eye-position sensitive. Once these cells were located in the light microscopic volume, we then needed to register the LM stack to the EM stack in order to locate the same cells in the EM volume. To do this, we made use of the fact that large, gross morphological features should be easy to spot in the EM stack.

Once enough such features were identified, we located these same landmarks in the high-res EM stack. Each pair of landmarks (one from the LM volume and one from the EM volume) was then used to calculate a global affine transform that was applied to transform the LM volume to be overlaid on the EM volume using the TrakEM2 plugin in Fiji [2]. Following this registration, we were able to reliable locate the same cells from the LM and the EM volumes.

Reconstructions

Two expert tracers reconstructed the cells beginning from the cell bodies in an independent manner. During the tracing process, one of the expert tracers annotated all pre and postsynaptic sites for each cells. The skeletonized tree structure was exported from TrakEM2 as *.swc files. These trees were then imported into Matlab using custom scripts to import .swc files as trees. The traces of the two tracers were compared by a third reviewer. The third reviewer, independently reviewed points of disagreement and decided which points of disagreement were either over-reconstructed or were under-reconstructed. In some cases, the traces were re-visited by the tracers if it was needed.

Analysis

All traces were exported as .swc files from TrakEM2. All tree lengths was reported as pathlengths unless noted otherwise. Similarly, all lengths to a pre or post synaptic site was reported as pathlengths. We defined the axon initiation site was annotated as the parent node of the first presynaptic site. For the putative-axons that originated at the soma, they were annotated as beginning from the root node. One cell from ipsi-only group was defined as an axon, based on diameter of the axons and the 'bare' initial segment. All neurites that were not axonal were

defied as dendritic. All nodes of the tree were thus divided as axonal nodes or dendritic nodes. Pathlengths were then generated for a tree over all axonal nodes or all dendritic nodes, and the length of the tree was the sum of all axonal length and dendritic length.

The diameter of the trees was generated by drawing a line segment across the cross-section of the tree at a random location along the tree. Many such line segments were drawn across the entire extent of the tree, where the tracer was blinded to the fact whether the neurite was an axon or a dendrite. The measurements were then separated as dendritic diameter or axonal diameter after all the trees were measured in this manner. The values were reported as a mean across all dendritic or axonal measures for a tree. A collateral was defined as all those segments of an axon, that emerged from the central axonal tree. All tree nodes that were axonal were then divided as those that were part of a collateral and those that were not. Following this, pathlengths and numbers were calculated by treating those nodes like any other. The completeness of cells was decided based on the number of neurites that exited the cells.

Arbor densities of the dendrites was computed by projecting all the axonal or dendritic nodes along the desired plane and reported in a normalized scale. Arbor volumes were computed using the Matlab function *convhull*. To infer the neurotransmitter identity from the stripe organization of the cell bodies, we annotated the location of all the cell bodies from a low-resolution stack. The cell density was then computed by projecting all the cells along the desired axis. This process picked out the peaks that were visible in the EM images. The location of a stripe was defined as the local peak that emerged from the cell density projecting analysis. The planar organization of the postsynapses and presynapses were fit to a plane using the *planefit* function, available on the Matlab central repository.

References

- [1] E Brustein, N Marandi, Y Kovalchuk, P Drapeau, and A Konnerth. "In vivo" monitoring of neuronal network activity in zebrafish by two-photon Ca²⁺ imaging. *Pflügers Archiv*, 446(6):766–773, 2003.
- [2] Albert Cardona, Stephan Saalfeld, Johannes Schindelin, Ignacio Arganda-Carreras, Stephan Preibisch, Mark Longair, Pavel Tomancak, Volker Hartenstein, and Rodney J Douglas. TrakEM2 software for neural circuit reconstruction. *PLoS ONE*, 7(6):e38011, 2012.
- [3] Kayvon Daie, Mark S Goldman, and Emre R F Aksay. Spatial patterns of persistent neural activity vary with the behavioral context of short-term memory. *Neuron*, 85(4):847–860, February 2015.
- [4] Kenneth J Hayworth, Josh L Morgan, Richard Schalek, Daniel R Berger, David G C Hildebrand, and Jeff W Lichtman. Imaging ATUM ultrathin section libraries with WaferMapper: a multi-scale approach to EM reconstruction of neural circuits. *Frontiers in Neural Circuits*, 8:68, 2014.
- [5] Andrew Miri, Kayvon Daie, Rebecca D Burdine, Emre Aksay, and David W Tank. Regression-Based Identification of Behavior-Encoding Neurons During Large-Scale Optical Imaging of Neural Activity at Cellular Resolution. *Journal of Neurophysiology*, 105(2):964–980, February 2011.
- [6] D Smetters, A Majewska, and R Yuste. Detecting action potentials in neuronal populations with calcium imaging. *Methods (San Diego, Calif.)*, 18(2):215–221, June 1999.
- [7] Juan Carlos Tapia, Narayanan Kasthuri, Kenneth J Hayworth, Richard Schalek, Jeff W Lichtman, Stephen J Smith, and JoAnn Buchanan. High-contrast en bloc staining of neuronal tissue for field emission scanning electron microscopy. *Nature Protocols*, 7(2):193–206, February 2012.